PROCEEDINGS OF SCIENCE

$B \to D^{(*)} \ell \nu$ form factors from $N_f = 2+1$ QCD with Möbius domain-wall quarks

JLQCD Collaboration: T. Kaneko[*a,b†], **Y. Aoki**[a], **B. Colquhoun**[a], **H. Fukaya**[c], **S. Hashimoto**[a,b]

[a] *High Energy Accelerator Research Organization (KEK), Ibaraki 305-0801, Japan*
[b] *School of High Energy Accelerator Science, SOKENDAI (The Graduate University for Advanced Studies), Ibaraki 305-0801, Japan*
[c] *Department of Physics, Osaka University, Osaka 560-0043, Japan*

We report on our study of the $B \to D^{(*)} \ell \nu$ semileptonic decays at zero and nonzero recoils in 2+1 flavor QCD. The Möbius domain-wall action is employed for light, charm and bottom quarks at lattice cutoffs $a^{-1} = 2.5$ and 3.6 GeV. We take bottom quark masses up to ≈ 2.4 times the physical charm mass to control discretization effects. The pion mass is as low as $M_\pi \sim 310$ MeV. We present our preliminary results for the relevant form factors and discuss the violation of heavy quark symmetry, which is a recent important isuue on the long-standing tension in the Cabibbo-Kobayashi-Maskawa matrix element $|V_{cb}|$ between the exclusive and inclusive decays.

The 36th Annual International Symposium on Lattice Field Theory - LATTICE2018
22-28 July, 2018
Michigan State University, East Lansing, Michigan, USA.

*Speaker.
†E-mail: takashi.kaneko@kek.jp

PoS(LATTICE2018)311

1. Introduction

The $B \to D^{(*)}\ell\nu$ semileptonic decays provide a determination of the Cabibbo-Kobayashi-Maskawa (CKM) matrix element $|V_{cb}|$. There has, however, been a long-standing tension with $|V_{cb}|$ from the inclusive decay [1], which has to be resolved towards an unambiguous interpretation of precise experimental data from forthcoming experiments at LHCb and Belle II. Lattice simulations play a central role in controlling theoretical uncertainties due to non-perturbative aspects of QCD [2]. So far, only a few modern studies have been performed for the $B \to D$ [3, 4] and $B \to D^*$ decays [5, 6, 7, 8] on gauge ensembles with staggered-type sea quarks. We also note that only preliminary results are available for $B \to D^*$ at nonzero recoil [6, 8].

The JLQCD Collaboration is pursuing a series of studies of B meson decays [9, 10, 11, 12] including the $B \to \pi\ell\nu$ [11] and inclusive decays [12], which are relevant to the tension in the CKM matrix elements. In this article, we report on our on-going calculation of the $B \to D^{(*)}$ form factors at zero and non-zero recoils.

2. Simulation

We simulate 2+1 flavor QCD using the tree-level improved Symanzik gauge action and the Möbius domain-wall quark action [13]. A careful choice of the detailed structure of the latter [14] enables us to preserve chiral symmetry to good accuracy at moderately large lattice cutoff $a^{-1} \simeq 2.5-4.5$ GeV. This simplifies the renormalization of the relevant weak currents. We simulate the strange quark mass m_s close to its physical value, whereas the degenerate up and down quark mass m_{ud} corresponds to pion masses as low as $M_\pi \sim 310$ MeV. In this article, we present our results at three combinations of (a^{-1}, m_{ud}, m_s) listed in Table 1. At each (a^{-1}, m_{ud}, m_s), the spatial lattice size L satisfies a condition $M_\pi L \gtrsim 4$ to control finite volume effects, and the statistics are 5,000 Molecular Dynamics time. We note that calculations at a larger cutoff $a^{-1} \sim 4.5$ GeV and a lighter $M_\pi \sim 230$ MeV are underway.

At the moderately large cutoffs $a^{-1} \geq 2.5$ GeV, we employ the same action for charm and bottom quarks. The charm quark mass m_c is set to its physical value, whereas we take bottom quark masses $m_b = 1.25^2 m_c$ and $1.25^4 m_c$ if $m_b \leq 0.8\, a^{-1}$. From our studies of the B and D meson (semi)leptonic decays [9, 11, 15], discretization errors are not expected to be large with this setup.

3. Form factors

The $B \to D$ decay proceeds only through the weak vector current V_μ due to parity symmetry of QCD, whereas the axial current A_μ also contributes to $B \to D^*$. The relevant matrix elements are

Table 1: Simulation parameters. $N_s^3 \times N_t \times N_5$ represents the five dimensional lattice size for the domain-wall formulation. Quark masses are bare value in lattice units.

β	$N_s^3 \times N_t \times N_5$	a^{-1}[GeV]	m_{ud}	m_s	M_π[MeV]	M_K[MeV]	m_b/m_c	$\Delta t + \Delta t'$
4.17	$32^3 \times 64 \times 12$	2.453(4)	0.019	0.040	499(1)	618(1)	1.25^2	24, 28
4.17	$32^3 \times 64 \times 12$	2.453(4)	0.007	0.040	309(1)	547(1)	1.25^2	22, 26
4.35	$48^3 \times 96 \times 8$	3.610(9)	0.012	0.025	501(2)	620(2)	1.25^2, 1.25^4	36, 42

parametrized by six form factors in total:

$$\sqrt{M_B M_D}^{-1}\langle D(p')|V_\mu|B(p)\rangle = (v+v')_\mu h_+(w)+(v-v')_\mu h_-(w), \tag{3.1}$$

$$\sqrt{M_B M_{D^*}}^{-1}\langle D^*(\varepsilon,p')|V_\mu|B(p)\rangle = \varepsilon_{\mu\nu\rho\sigma}\,\varepsilon^{*\nu}v'^{\rho}v^{\sigma}\,h_V(w), \tag{3.2}$$

$$\sqrt{M_B M_{D^*}}^{-1}\langle D^*(\varepsilon,p')|A_\mu|B(p)\rangle = -i(w+1)\,\varepsilon^*_\mu\,h_{A_1}(w)+i(\varepsilon^*v)\,v_\mu\,h_{A_2}(w)+i(\varepsilon^*v)\,v'_\mu\,h_{A_3}(w), \tag{3.3}$$

where $v=p/M_B$ and $v'=p'/M_{D^{(*)}}$ are the four velocity of B and $D^{(*)}$, $w=vv'$ is the recoil parameter, and ε is the polarization vector of D^* satisfying $\varepsilon p'=0$. In this study, the B meson is at rest ($\mathbf{p}=\mathbf{0}$), and we change the three momentum of $D^{(*)}$ as $|\mathbf{p}'|^2=0,1,2,3$ (in units of $(2\pi/L)^2$) to study the w dependence of the form factors.

These matrix elements can be extracted from the asymptotic behavior of three-point functions

$$\begin{aligned}
&C^{BD^{(*)}}_{\mathcal{O}_\Gamma}(\Delta t,\Delta t';\mathbf{p},\mathbf{p}')\\
&= \frac{1}{N_{t_{\rm src}}}\sum_{t_{\rm src}}\sum_{\mathbf{x}_{\rm src},\mathbf{x},\mathbf{x}'}\langle\mathcal{O}_{D^{(*)}}(\mathbf{x}',t_{\rm src}+\Delta t+\Delta t')\mathcal{O}_\Gamma(\mathbf{x},t_{\rm src}+\Delta t)\mathcal{O}_B(\mathbf{x}_{\rm src},t_{\rm src})^\dagger\rangle e^{-i\mathbf{p}(\mathbf{x}-\mathbf{x}_{\rm src})-i\mathbf{p}'(\mathbf{x}'-\mathbf{x})}\\
&\to \frac{Z^*_{D^{(*)}}(\mathbf{p}')\,Z_B(\mathbf{p})}{4E_{D^{(*)}}(\mathbf{p}')E_B(\mathbf{p})}\langle D^{(*)}(p')|\mathcal{O}_\Gamma|B(p)\rangle e^{-E_{D^{(*)}}(\mathbf{p}')\Delta t'-E_B(\mathbf{p})\Delta t}\quad(\Delta t,\Delta t'\to\infty),
\end{aligned} \tag{3.4}$$

where $\mathcal{O}_\Gamma=V_\mu$ or A_μ, and the argument ε is suppressed for Z_{D^*} and $|D^*(p')\rangle$. Gaussian smearing is applied to the interpolating field $\mathcal{O}_P$ ($P=B,D,D^*$) to enhance its overlap to the ground state $Z_P(\mathbf{p})=\langle P(p)|\mathcal{O}_P^\dagger\rangle$. We take two values of the total temporal separation $\Delta t+\Delta t'$ listed in Table 1 to check whether the excited contamination is sufficiently suppressed. The two-point function

$$C^P(\Delta t;\mathbf{p}) = \frac{1}{N_{t_{\rm src}}}\sum_{t_{\rm src}}\sum_{\mathbf{x}_{\rm src},\mathbf{x}}\langle\mathcal{O}_P(\mathbf{x},t_{\rm src}+\Delta t)\mathcal{O}_P(\mathbf{x}_{\rm src},t_{\rm src})^\dagger\rangle e^{-i\mathbf{p}(\mathbf{x}-\mathbf{x}_{\rm src})}\to\frac{|Z_P(\mathbf{p})|^2}{2E_P(\mathbf{p})}e^{-E_P(\mathbf{p})\Delta t} \tag{3.5}$$

is also measured to estimate the rest mass M_P, energy E_P and the overlap factor Z_P ($P=B,D,D^*$).

We improve the statistical accuracy of the three- and two-point functions, $C^{BD^{(*)}}_{\mathcal{O}_\Gamma}$ and C^P, by averaging over the source location $(\mathbf{x}_{\rm src},t_{\rm src})$. For the temporal location $t_{\rm src}$, we simply repeat our calculation at two different time-slices (hence, $N_{t_{\rm src}}=2$ in Eqs. (3.4) and (3.5)). The summation over the spatial location $\mathbf{x}_{\rm src}$ is implemented by using the volume source with Z_2 noise. We also average $C^{BD^{(*)}}_{\mathcal{O}_\Gamma}$ and C^P over the momentum configurations, which are equivalent due to rotational and parity symmetries. These procedures improve the statistical accuracy by factor of 2–4 with our simulation setup.

We construct ratios of $C^{BD^{(*)}}_{\mathcal{O}_\Gamma}$ and C^P for a more precise and reliable calculation of the form factors. The double ratios without nonzero momentum [16]

$$R^{BD^{(*)}}_{1(i)}(\Delta t,\Delta t') = \frac{C^{BD^{(*)}}_{V_4(A_i)}(\Delta t,\Delta t';\mathbf{0},\mathbf{0})\,C^{D^{(*)}B}_{V_4(A_i)}(\Delta t,\Delta t';\mathbf{0},\mathbf{0})}{C^{BB}_{V_4(A_i)}(\Delta t,\Delta t';\mathbf{0},\mathbf{0})\,C^{DD}_{V_4(A_i)}(\Delta t,\Delta t';\mathbf{0},\mathbf{0})}\xrightarrow[\Delta t,\Delta t'\to\infty]{}|h_{+(A_1)}(1)|^2 \tag{3.6}$$

give an accurate estimate of h_+ and h_{A_1} at zero recoil $w=1$, which are important inputs in the conventional determination of $|V_{cb}|$. The analysis of h_+ and h_- at nonzero recoil $w>1$ is analogous

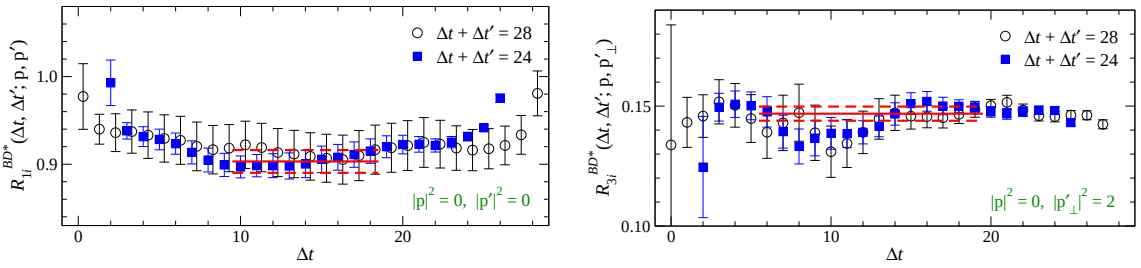

Figure 1: Ratios of three-point functions for $B \to D^*$. The left and right panels show $R_{1i}^{BD^*}(\Delta t, \Delta t'; \mathbf{0}, \mathbf{0})$ and $R_{3i}^{BD^*}(\Delta t, \Delta t'; \mathbf{0}, \mathbf{p}'_\perp)$, respectively, as a function of Δt. We plot data at $\beta = 4.17$ and $(m_{ud}, m_s) = (0.019, 0.040)$. The open circles and filled squares show data with $\Delta t + \Delta t' = 28$ and 24, respectively. The red horizontal lines show a constant fit to data with $\Delta t + \Delta t' = 24$.

to our study of $K \to \pi$ and previous studies of $B \to D$ [17, 3, 4]. Together with ratios

$$R_2^{BD}(\Delta t, \Delta t'; \mathbf{0}, \mathbf{p}') = \frac{C_{V_4}^{BD}(\Delta t, \Delta t'; \mathbf{0}, \mathbf{p}') C^D(\Delta t', \mathbf{0})}{C_{V_4}^{BD}(\Delta t, \Delta t'; \mathbf{0}, \mathbf{0}) C^D(\Delta t', \mathbf{p}')} \to \frac{(1+w)h_+(w) + (1-w)h_-(w)}{2h_+(1)}, \quad (3.7)$$

$$R_{3i}^{BD}(\Delta t, \Delta t'; \mathbf{0}, \mathbf{p}') = \frac{C_{V_i}^{BD}(\Delta t, \Delta t'; \mathbf{0}, \mathbf{p}')}{C_{V_4}^{BD}(\Delta t, \Delta t'; \mathbf{0}, \mathbf{p}')} \to v'_i \frac{h_+(w) - h_-(w)}{(1+w)h_+(w) + (1-w)h_-(w)}, \quad (3.8)$$

we can reconstruct the form factors as

$$h_{+(-)}(w) = \sqrt{R_1^{BD}} R_2^{BD} \left\{ 1 \pm (1 \mp w) \frac{R_{3i}^{BD}}{v'_i} \right\}. \quad (3.9)$$

The analysis of $B \to D^*$ is slightly more involved, and we need to distinguish the D^* momentum $\mathbf{p}'_\not{}$, which induces $\varepsilon v \neq 0$ through the convention $\varepsilon p' = 0$, and $\mathbf{p}'_\perp$ leading to $\varepsilon v = 0$ (note that $\mathbf{v} = \mathbf{0}$ in this study). The w-dependence of h_{A_1} can be studied by a ratio similar to (3.7) with A_i and $\mathbf{p}'_\perp$

$$R_{2i}^{BD^*}(\Delta t, \Delta t'; \mathbf{0}, \mathbf{p}'_\perp) = \frac{C_{A_i}^{BD^*}(\Delta t, \Delta t'; \mathbf{0}, \mathbf{p}'_\perp) C^{D^*}(\Delta t, \mathbf{0})}{C_{A_i}^{BD^*}(\Delta t, \Delta t'; \mathbf{0}, \mathbf{0}) C^{D^*}(\Delta t, \mathbf{p}'_\perp)} \to \frac{1+w}{2} \frac{h_{A_1}(w)}{h_{A_1}(1)}, \quad (3.10)$$

whereas a ratio $C_{A_{\{i,4\}}}^{BD^*}(\Delta t, \Delta t'; \mathbf{0}, \mathbf{p}'_\not{})/C_{A_i}^{BD^*}(\Delta t, \Delta t'; \mathbf{0}, \mathbf{p}'_\perp)$ is sensitive to h_{A_2} and h_{A_3} at $w > 1$ [6]. A form factor ratio $R_1(w) = h_V(w)/h_{A_1}(w)$ is a key quantity in recent phenomenological discussions about the tension in $|V_{cb}|$, and is determined from

$$R_{3i}^{BD^*}(\Delta t, \Delta t'; \mathbf{0}, \mathbf{p}'_\perp) = \frac{C_{V_i}^{BD^*}(\Delta t, \Delta t'; \mathbf{0}, \mathbf{p}'_\perp)}{C_{A_i}^{BD^*}(\Delta t, \Delta t'; \mathbf{0}, \mathbf{p}'_\perp)} \to \frac{\varepsilon_{ijk} \varepsilon_j^* v'_{\perp k}}{1+w} \frac{h_V(w)}{h_A(w)}. \quad (3.11)$$

We average $C_{V_i}^{BD^{(*)}}$ and $C_{A_i}^{BD^*}$ over $i = 1, 2, 3$ with appropriately rotated $\mathbf{p}'$ and $\mathbf{p}'_\not{}$ before calculating the above ratios. Note that renormalization factors cancel even in the ratio (3.11) due to chiral symmetry preserved in our simulations.

Figure 1 shows an example of the ratios for $B \to D^*$. We confirm reasonable consistency between two sets of data with different values of $\Delta t + \Delta t'$ suggesting that the excited state contamination is sufficiently suppressed. The statistical accuracy with the smaller value of $\Delta t + \Delta t' \approx 1.8$ fm is typically $2-6$ % for h_+, h_{A_1}, h_{A_3}, h_V, which are reduced to the Isgur-Wise function $\xi(w)$ with the

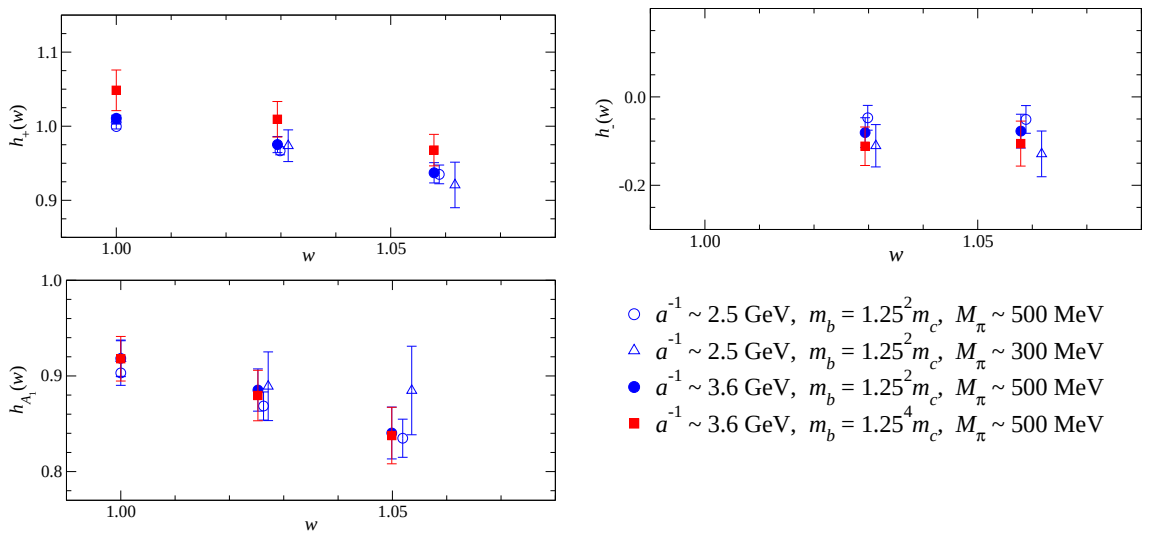

Figure 2: Form factors as a function of w. We plot h_+, h_- and h_{A_1} in the top-left, top-right and bottom-left panels, respectively. The blue (red) symbols show data with $m_b = 1.25^2 m_c$ ($1.25^4 m_c$), whereas the open (filled) symbols are at $a^{-1} \simeq 2.5$ (3.6) GeV.

normalization $\xi(1) = 1$ in the heavy quark limit $m_c, m_b \to \infty$. Other form factors h_- and h_{A_2} vanish in the heavy quark limit, and their results are close to zero with a typical accuracy of $\lesssim 50\,\%$.

Figure 2 shows results for h_+, h_- and h_{A_1} at different simulation points as a function of w. These form factors describe the differential decay rates at zero recoil $d\Gamma/dw(B \to D^{(*)}\ell\nu)|_{w=1}$ for the massless lepton $m_\ell = 0$. These and other form factors mildly depend on a^{-1}, m_b and M_π – at least in our simulation range of these parameters. We note that similar mild dependence on a^{-1} and m_b is also observed for the $B \to \pi\ell\nu$ form factors [11]. While all the form factors have to be extrapolated to the continuum limit and physical up, down and bottom quark masses, the mild dependence may suggest that the preliminary results are not far from these limits and the extrapolation can be reasonably controlled.

4. Heavy quark symmetry violation and $|V_{cb}|$

The $B \to D^*\ell\nu$ differential decay rate for $m_\ell = 0$ is described by three combinations of the form factors, h_{A_1}, h_V and $h_{A_2} + r h_{A_3}$ ($r = M_{D^*}/M_B$). Boyd, Grinstein and Lebed (BGL) proposed a model independent parametrization [18], which Taylor-expands the (regularized) form factors around zero recoil in $w-1$, or in terms of a small kinematical parameter $z = (\sqrt{w+1} - \sqrt{2}a)/(\sqrt{w+1} + \sqrt{2}a)$ with a a tunable input. While one can derive constraints on the expansion parameters from unitarity, they are rather weak. The conventional determination of $|V_{cb}|$ therefore employs the Caprini-Lellouch-Neubert (CLN) parametrization [19], which has only four free parameters: the normalization and slope of h_{A_1}, $R_1(1) = h_V(1)/h_{A_1}(1)$ and $R_2(1) = \{h_{A_2}(1) + r h_{A_3}(1)\}/h_{A_1}(1)$. The remaining parameters are constrained by next-to-leading order (NLO) heavy quark effective theory (HQET) with QCD sum rule inputs for the sub-leading Isgur-Wise functions. Recently, Belle has published a preliminary analysis of the differential decay rate with unfolded kinematical and angular distri-

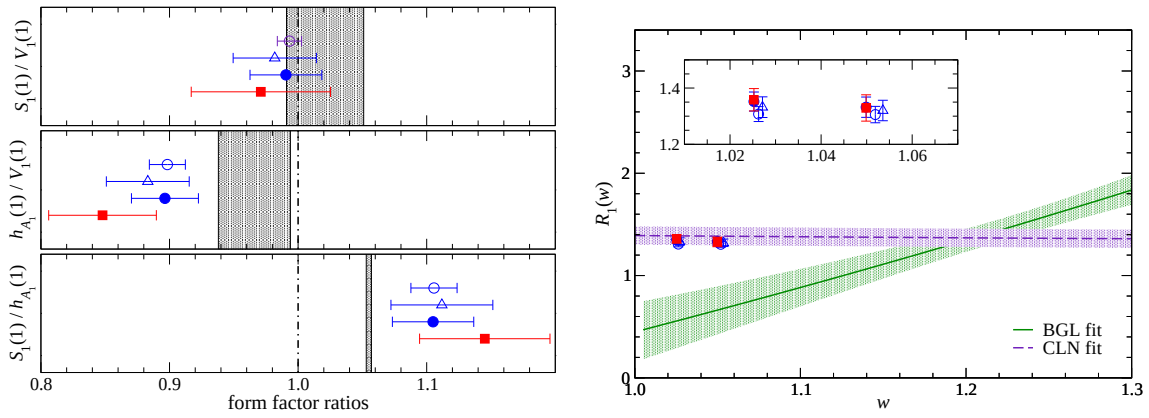

Figure 3: Left panel: form factor ratios $S_1(1)/V_1(1)$ (left-top panel), $h_{A_1}(1)/V_1(1)$ (left-middle panel) and $S_1(1)/h_{A_1}(1)$ (left-bottom panel). These ratios are unity in the heavy quark limit, and the shaded region shows the NLO HQET estimate [26]. Right panel: $R_1(w)$ as a function of w. The BGL and CLN fits shown in the green and purple bands, respectively, are from Ref. [25] by courtesy of the authors. The inner panel magnifies a small region around our lattice results. In all the panels, our results are plotted by the same symbols as Fig. 2.

butions for the first time [20][1]. This allows a determination based on the BGL parametrization yielding $|V_{cb}|\times 10^3 = 41.7(^{+2.0}_{-2.1})$ [22] and $41.9(^{+2.0}_{-1.9})$ [23], which are compatible with the inclusive determination 42.0(0.5) and slightly larger than 38.2(1.5) with the CLN parametrization [20]. This led to recent phenomenological discussions about higher order correction to NLO HQET [24, 25].

In the left panel of Fig. 3, we compare form factor ratios between lattice QCD and NLO HQET. We again confirm that our lattice results mildly depend on a^{-1}, m_b and M_π. There seems to be a systematic deviation for $h_{A_1}/V_1(1)$ and $S_1(1)/h_{A_1}(1)$, where $V_1 = h_+ - (1-r)h_-/(1+r)$ and $S_1 = h_+ - (1+r)(w-1)h_-/(1-r)(w+1)$ are vector and scalar form factors for $B \to D\ell\nu$. Note that the CLN constraint on h_{A_1} is derived from $h_{A_1}(w)/V_1(w)$ in NLO HQET and the unitarity bound for $V_1(w)$ for $B \to D\ell\nu$ [19]. Our observation suggests that NLO HQET may receive significant higher order corrections as discussed in Ref. [24].

However, this seems not to be the case for $R_1(w)$, which exhibits one of the largest differences between the CLN and BGL analyses [25]. The right panel of Fig. 3 shows that our results for $R_1(w)$ favor the CLN prediction, though they eventually have to be extrapolated to the continuum limit and the physical quark masses. These observations suggest that, at the moment, the $|V_{cb}|$ tension may not be simply attributed to the higher order corrections to NLO HQET, and more lattice data are welcome for a more detailed comparison between the CLN and BGL analyses.

5. Outlook

In this article, we report on our study of the $B \to D^{(*)}\ell\nu$ decays at zero and nonzero recoils. With our simulation setup, the relevant form factors show mild dependence on a^{-1}, m_b and M_π, which led us to discuss implication of the preliminary results to the $|V_{cb}|$ tension. Our goal is to

[1] Reference [20] analyzes results with a tagged approach. We note that, after the conference, Belle updated their analysis of $B \to D^*\ell\nu$ with an untagged approach by using both the BGL and CLN parametrizations [21].

obtain purely theoretical prediction for the form factors through lattice simulations and a model-independent parametrization such as BGL towards a more reliable determination of $|V_{cb}|$. To this end, we are planning to extend our simulation to a lighter pion mass $M_\pi \sim 230$ MeV, a finer lattice with $a^{-1} \sim 4.5$ GeV and $m_b = 1.25^5 m_c$ for a controlled extrapolation of our results to the continuum limit and physical m_{ud} and m_b. Our data at different m_b's are expected to be useful to test the heavy quark scaling for the form factors given by heavy quark symmetry.

We are grateful for F.U. Bernlochner, Z. Ligeti, M. Papucci, and D.J. Robinson for making their numerical results in Ref. [25] available to us. Numerical simulations are performed on Oakforest-PACS at JCAHPC under a support of the HPCI System Research Projects (Project IDs: hp170106 and hp180132) and Multidisciplinary Cooperative Research Program in CCS, University of Tsukuba (Project IDs: xg17i036 and xg18i016). This work is supported in part by JSPS KAKENHI Grant Numbers 16K05320, 18H01216, 18H03710 and 18H04484.

References

[1] Y. Amhis *et al.* (Heavy Flavor Averaging Group), Eur. Phys. J. C77 (2017) 895.
[2] For a recent review, see S. Hashimoto, PoS (LATTICE2018) 008 in these proceedings.
[3] J.A. Bailey *et al.* (Fermilab and MILC Collaboration), Phys. Rev. D 92 (2015) 034506.
[4] H. Na *et al.* (HPQCD Collaboration), Phys. Rev. D 92 (2015) 054510.
[5] J.A. Bailey *et al.* (Fermilab and MILC Collaboration), Phys. Rev. D 89 (2014) 114504 (2014).
[6] A. Vaquero Avilés-Casco *et al.* (Fermilab and MILC Collaboration), EPJ Web Conf. 175 (2018) 13003.
[7] J. Harrison *et al.* (HPQCD Collaboration), Phys. Rev. D 97 (2018) 054502.
[8] A. Vaquero Avilés-Casco *et al.* (Fermilab and MILC Collaboration), PoS (LATTICE2018) 282 in these proceedings.
[9] B. Fahy *et al.* (JLQCD Collaboration), PoS (LATTICE2015) 074.
[10] K. Nakayama and S. Hashimoto (JLQCD Collaboration), PoS (LATTICE2018) 221 in these proceedings.
[11] B. Colquhoun *et al.* (JLQCD Collaboration), PoS (LATTICE2018) 274 in these proceedings.
[12] S. Hashimoto *et al.* (JLQCD Collaboration), PoS (LATTICE2018) 307 in these proceedings.
[13] R.C. Brower, H. Neff and K. Orginos, Nucl. Phys. (Proc.Suppl.) 140 (2005) 686.
[14] T. Kaneko *et al.* (JLQCD Collaboration), PoS (LATTICE 2013) 125.
[15] T. Kaneko *et al.* (JLQCD Collaboration), EPJ Web Conf. 175 (2018) 13007.
[16] S. Hashimoto *et al.*, Phys. Rev. D61 (1999) 014502.
[17] S. Aoki *et al.* (JLQCD Collaboration), Phys. Rev. D96 (2017) 034501.
[18] C.G. Boyd, B. Grinstein and R.F. Lebed, Phys. Rev. D56 (1997) 6895.
[19] I. Caprini, L. Lellouch, M. Neubert, Nucl. Phys. B530 (1998) 153.
[20] A. Abdesselam *et al.* (Belle Collaboration), arXiv:1702.01521 [hep-ex].
[21] A. Abdesselam *et al.* (Belle Collaboration), arXiv:1809.03290 [hep-ex].
[22] D. Bigi, P. Gambino and S. Schacht, Phys. Lett. B769 (2017) 441.
[23] B. Grinstein and A. Kobach, Phys. Lett. B771 (2017) 359.
[24] D. Bigi, P. Gambino and S. Schacht, JHEP 11 (2017) 061.
[25] F.U. Bernlochner, Z. Ligeti, M. Papucci and D.J. Robinson, Phys. Rev. D96 (2017) 091503.
[26] F.U. Bernlochner, Z. Ligeti, M. Papucci, and D.J. Robinson, Phys. Rev. D 95 (2017) 115008.